Title

Single-cell nanobiopsy reveals compartmentalization of mRNAs within neuronal cells

Journal

Journal of Biological Chemistry, 293(13)

ISSN

0021-9258

Authors

Tóth, Eszter N
Lohith, Akshar
Mondal, Manas
et al.

Publication Date

2018-03-01

DOI

10.1074/jbc.m117.800763

Peer reviewed

Single-cell nanobiopsy reveals compartmentalization of mRNAs within neuronal cells

Received for publication, June 6, 2017, and in revised form, January 21, 2018 Published, Papers in Press, January 29, 2018, DOI 10.1074/jbc.M117.800763

Eszter N. Tóth[‡§¶], Akshar Lohith[¶], Manas Mondal[‖], Jia Guo[‖], Akiyoshi Fukamizu[‡§], and Nader Pourmand[¶1]

From the [‡]Ph.D. Program in Human Biology, School of Integrative and Global Majors and the [§]Life Science Center, Tsukuba Advanced Research Alliance, Department of Life and Environmental Sciences, University of Tsukuba, Ibaraki 305-8577, Japan, the [¶]Department of Biomolecular Engineering, Jack Baskin School of Engineering, University of California at Santa Cruz, Santa Cruz, California 95064, and the [‖]Department of Chemistry and Biochemistry & Biodesign Institute, Arizona State University, Tempe, Arizona 85287

Edited by Ronald C. Wek

In highly polarized cells such as neurons, compartmentalization of mRNA and of local protein synthesis enables remarkably fast, precise, and local responses to external stimuli. These responses are highly important for neuron growth cone guidance, synapse formation, and regeneration following injury. Because an altered spatial distribution of mRNA can result in mental retardation or neurodegenerative diseases, subcellular transcriptome analysis of neurons could be a useful tool for studying these conditions, but current techniques, such as *in situ* hybridization, bulk microarray, and RNA-Seq, impose tradeoffs between spatial resolution and multiplexing. To obtain a comprehensive analysis of the cell body *versus* neurite transcriptome from the same neuron, we have recently developed a label-free, single-cell nanobiopsy platform based on scanning ion conductance microscopy that uses electrowetting within a quartz nanopipette to extract cellular material from living cells with minimal disruption of the cellular membrane and milieu. In this study, we used this platform to collect samples from the cell bodies and neurites of human neurons and analyzed the mRNA pool with multiplex RNA sequencing. The minute volume of a nanobiopsy sample allowed us to extract samples from several locations in the same cell and to map the various mRNA species to specific subcellular locations. In addition to previously identified transcripts, we discovered new sets of mRNAs localizing to neurites, including nuclear genes such as *Eomes* and *Hmgb3*. In summary, our single-neuron nanobiopsy analysis provides opportunities to improve our understanding of intracellular mRNA transport and local protein composition in neuronal growth, connectivity, and function.

This work was supported in part by National Institutes of Health Grant P01-35HG000205; NINDS, National Institutes of Health Grant R21NS082927; the National Institutes of Health's Follow the Same Cell Prize; and Grants-in-Aid for Scientific Research on Innovative Areas (23116001 and 23116004) from MEXT (Ministry of Education, Culture, Sports, Science and Technology), Japan. The authors declare that they have no conflicts of interest with the contents of this article. The content is solely the responsibility of the authors and does not necessarily represent the official views of the National Institutes of Health.

This article contains Tables S1–S9 and Figs. S1–S4.

The data discussed in this publication have been deposited in NCBI's Gene Expression Omnibus and are accessible through GEO Series accession number GSE103461.

[1] To whom correspondence should be addressed: Dept. of Biomolecular Engineering, Jack Baskin School of Engineering, University of California at Santa Cruz, 1156 High St., Santa Cruz, CA 95064. Tel.: 831-502-7315; E-mail: pourmand@soe.ucsc.edu.

In highly polarized cells, such as neurons, compartmentalization of mRNA and local protein synthesis is implemented in rapid, remarkably precise, local responses to external stimuli, allowing tight and accurate regulation of subcellular composition and content (1). This implies that at each subcellular compartment, the amount of specific proteins depends on the local rate of translation rather than the absolute amount of mRNA (*i.e.* transcription) (2). So far, analysis of mRNA species in dendrites and axons has revealed thousands of transcripts that are differentially localized (3–7). Some sequence motifs at the 3′-UTR, 5′-UTR, and retained intron regions of the mRNA have been found to regulate the localization of transcripts to neuronal processes (8, 9) in the translationally repressed state during mRNA trafficking (1). In addition, mRNA transport and local translation are involved in different aspects of neuronal homeostasis, such as growth cone guidance (10, 11), axon maintenance (12), injury response (13), and synapse and memory formation (14). Altered mRNA transport and translation can result in devastating consequences, including mental retardation or neurodegenerative disease, such as amyotrophic lateral sclerosis (15).

Comparative subcellular transcriptome analysis of neurons has faced many technical limitations. To detect genes specific for the axons or dendrites, the neurites must be separated from the soma. This can be achieved either by culturing neurons in compartmentalized chambers (3, 4); microdissection of specific brain areas where the cells have highly ordered, uniform arrangement, *e.g.* the CA1 region of the hippocampus (5); or laser microdissection and glass micropipette aspiration of neurites of cultured neurons (16–19). Currently available techniques (such as *in situ* hybridization, bulk microarray, or RNA sequencing) impose a tradeoff between spatial resolution and multiplexing; *in situ* hybridization can visualize only a few kinds of transcripts at a time, whereas when tissue, cells, or whole neurites are harvested for multiplexed microarray or RNA sequencing, all spatial information is lost. In addition, previous studies used different cell types for axonal and dendritic transcriptome analysis, making data comparison very difficult. There was no available method for multiplexed, neurite transcriptome analysis at the single-cell level. Our group recently developed a label-free, single-cell nanobiopsy platform based

on scanning ion conductance microscopy (SICM),[2] which uses electrowetting within a quartz nanopipette to extract cellular material from living cells with minimal disruption of the membrane and cellular milieu. Using electron microscopic measurements and geometrical calculations, this volume was estimated to be ~50 fl, which corresponds to ~1% of the volume of a cell (20).

In this study, we used our nanobiopsy platform to extract samples from the soma and neurites of human induced pluripotent cell-derived iCell® neurons and analyzed the mRNA pool by multiplex RNA sequencing. Because of the minute volume of a nanobiopsy sample, it was possible to extract cytoplasm from multiple locations in one cell. We found that the subcellular mRNA pools showed great mosaicism and that cell regions are fundamentally different from each other in terms of their mRNA composition. Neuronal cell bodies showed enrichment for transcripts encoding proteins involved in transcriptional regulation and protein transport, whereas neurites were enriched in genes related to protein synthesis, protein targeting to endoplasmic reticulum (ER), and mRNA metabolism. In addition to the previously identified transcripts, we report a new set of mRNAs that specifically localize to neurites, including mRNAs encoding proteins that were previously believed to localize exclusively to the nucleus. Here we provide evidence that single-neuron nanobiopsy studies can deepen our understanding of mRNA compartmentalization and open the possibility to study the molecular mechanism for specific neuronal functions, cellular circuitry, neuronal growth, and network formation.

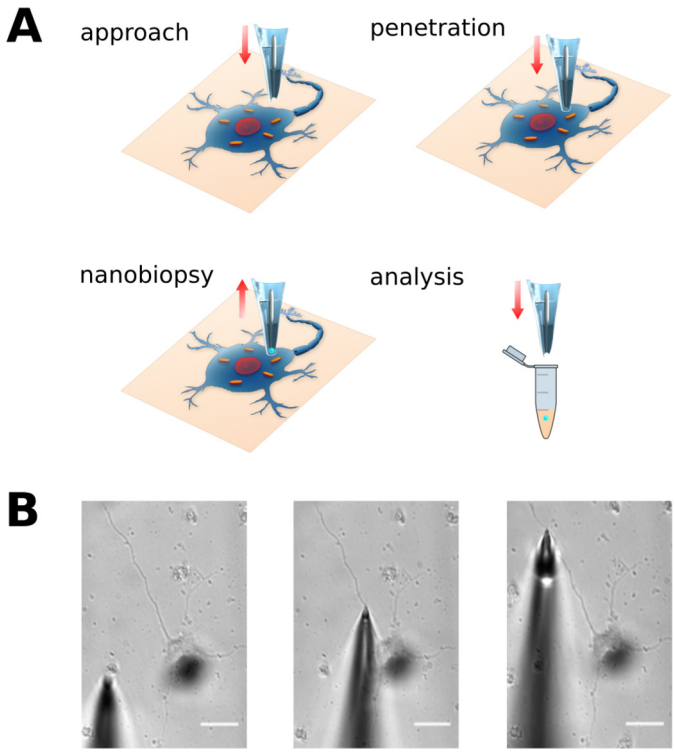

Figure 1. Schematic of single cell nanobiopsy. *A*, illustration of automated approach to cell surface, penetration in the cell cytosol, followed by controlled aspiration of cytoplasmic material by electrowetting. *B*, optical micrographs of a neuronal cell projection nanobiopsy procedure illustrating the cell membrane penetration and aspiration via electrowetting. Two nanobiopsy samples were collected from the same neuronal projection. *Scale bars*, 25 μm.

Results

Nanobiopsy sampling of neuronal cells

To study the spatial pattern of mRNA compartmentalization within neuronal cells, we extracted samples from the cell bodies and neurites of neurons using our nanobiopsy platform. The SICM–based setup maps the cell surface by measuring the ion current flowing through a quartz nanopipette. Our custom-coded control software enables automatic cell surface finding, penetration, and aspiration of cellular material through electrowetting (Fig. 1). The aspiration volume is ~50 fl, corresponding to 1% of the cell's total volume. Our method of sampling causes minimal damage to the cells such that cell viability is maintained and thus several samples can be collected repeatedly from the same cell (20). We collected 43 nanobiopsy samples from 33 cells in total, of which 13 samples were derived from cell bodies and 30 from neurites (Table S1). The cDNA was prepared from each individual sample for library preparation. Altogether, we generated 43 single-nanobiopsy RNA-sequencing libraries. Because of the minute amount of input RNA used, the sequencing depth ranged between 10 and 2900 mapped reads per nanobiopsy sample.

The timing of nanobiopsy can be controlled by adjusting the voltage applied to the electrode, targeting a very small subcellular region, with practically no contamination from other sources. Thus, even genes displaying a low number of reads mapped uniquely to an annotated transcript may be scored positive for expression. To confirm this, we prepared negative control sequencing libraries from External RNA Controls Consortium (ERCC) RNA Spike-In Mix RNAs (Ambion) without adding any RNA derived from nanobiopsy samples. The controls consist of a set of unlabeled, polyadenylated transcripts designed to be added to an RNA analysis experiment after sample isolation, to infer library quality (21). Contrary to our nanobiopsy sequencing libraries, we had very few reads mapped to human genome (Table S2, Sample_NC). As for the false negatives, we must consider the following two things. ERCC RNA Spike-In Mix was added to each nanobiopsy sample for quality control and sensitivity check (Fig. S1*A*). After RNA sequencing read mapping and analysis of the ERCC reads, we found that the lower limit of reliable detection is ~50–100 mRNA copies (Fig. S1*B*). Thus, if a nanobiopsy sample contains less than 50–100 copies of a transcript, it is likely that it will not be detected and will be a false negative.

We considered genes to have higher expression level if they had at least four reads mapped in a nanobiopsy sample (approximately the top 20% of genes). Mapping of the sequencing reads to the human genome identified 10–1000 genes expressed in each sample (Fig. 2, *A* and *B*, and Table S2). This very wide range indicates that the concentration and/or homogeneity of mRNA transcripts vary greatly depending on the precise subcellular location. The total number of genes found in all 43

[2] The abbreviations used are: SICM, scanning ion conductance microscopy; ER, endoplasmic reticulum; SOM, self-organizing map; GO, Gene Ontology Enrichment Analysis; RNA-seq, RNA sequencing; SSC, saline-sodium citrate.

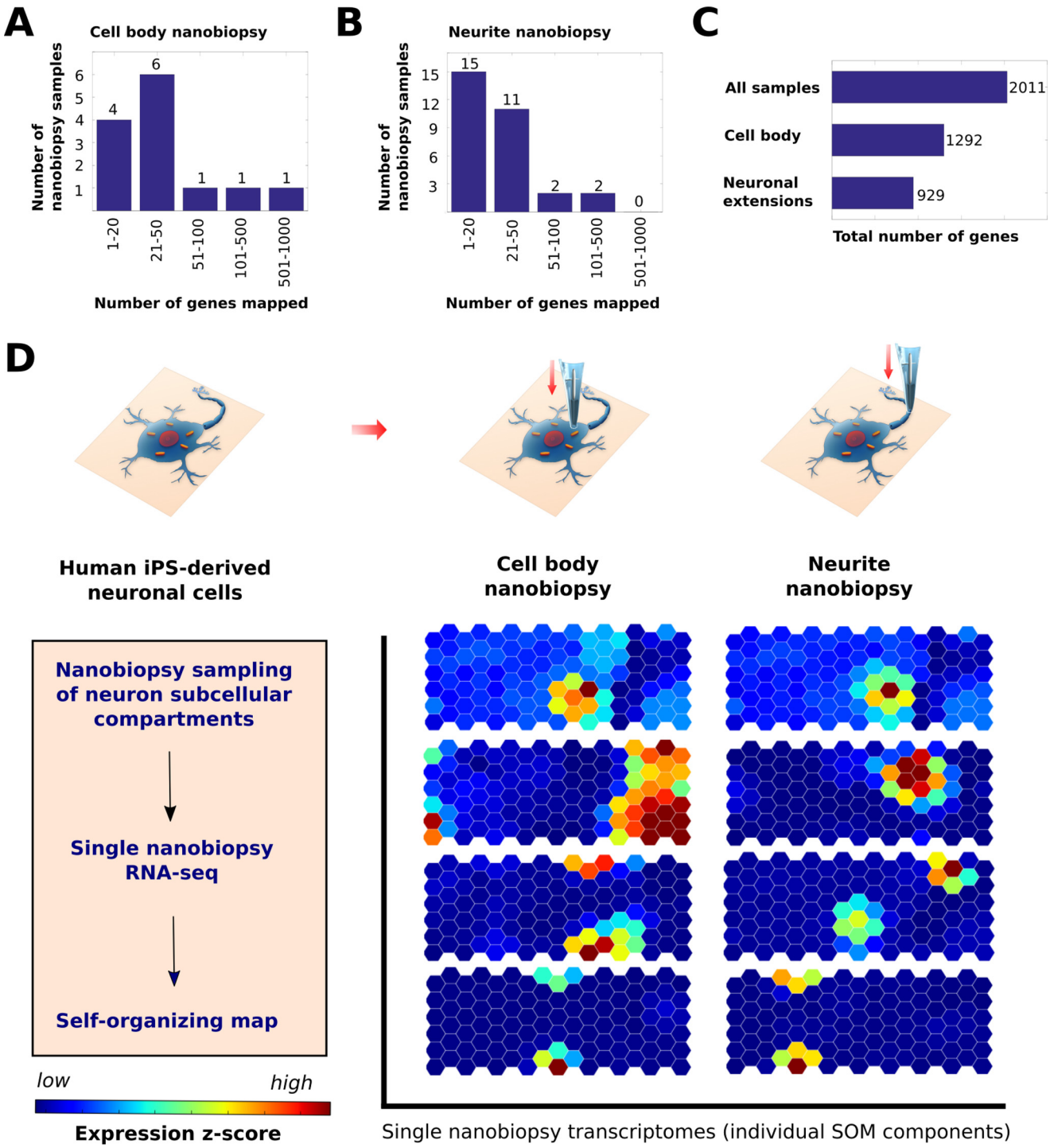

Figure 2. Neuronal cell nanosurgery RNA-seq read mapping. *A* and *B*, histogram of the number of mRNA transcripts mapped by analyzing the nanobiopsy samples taken from cell body (*A*) of neuronal processes (*B*) of neuronal cells. *C*, the total number of mRNA transcripts detected in all nanobiopsy samples, all cell body samples, and all neurite samples. *D*, schematic illustration of nanobiopsy sampling from neurons and RNA-seq analysis using the SOM. Briefly, the 1000 genes with the greatest variance among the libraries were used for training a self-organizing map, where each *hexagon* represents a group of genes whose expression patterns across samples are most similar. These units are clustered and are located in the same positions across all nanobiopsy components of the SOM. Thus, in this 2D heat map, spatial proximity corresponds to expression pattern similarity. Each nanobiopsy transcriptome can be visualized as a component of SOM, by thus mapping the genes expressed onto the SOM. Four representative nanobiopsy transcriptome SOM components are shown for each subcellular compartment.

nanobiopsy samples was 2011, of which approximately ~1300 mRNA transcripts were identified in cell bodies and ~930 in neuronal processes (Fig. 2*C* and Table S3). The list of the most abundant transcripts based on the number of nanobiopsies in which they were detected can be seen in Table S4. Previously, other groups have used laser microdissection or aspiration by glass pipette to collect individual neurites from cultured neurons for transcriptome analysis. Zivraj *et al.* (16) used laser-capture microdissection to collect axon segments. After pooling 250 axon segments and microarray analysis, they identified

~5000 transcripts that localize to axon. Francis *et al.* (18) used glass micropipette to collect a pool of 100–400 dendrites for microarray analysis and found ~11,000 genes in dendrites. The advantage of neurite microdissection compared with bulk sampling was that contamination from cell body could be reduced very significantly. The most important difference between microdissection and nanobiopsy sampling is the amount of sample being collected. When hundreds of whole neurites are dissected and pooled, a large amount of input material is present; therefore a high number of transcripts can be identified. A single nanobiopsy, however, collects ~1% of the volume of a cell. This enables us to collect samples from very small, targeted area. The number of transcripts sequenced is smaller compared with microdissection sampling, but we can get a much higher spatial resolution. In addition, the cell viability does not decrease after the procedure, allowing us to collect multiple small samples from the same cell.

We analyzed this high dimensional data set using the self-organizing map (SOM) described by Kim *et al.* (23). The SOM provides an intuitive way to visualize and examine the repertoire of genes in each nanobiopsy sample. We mapped 2011 genes onto a SOM, where each hexagon represents a set of genes whose expression patterns are most similar to one another. These units are clustered and located in the same positions across all nanobiopsy components of the SOM. Thus, in this 2D heat map, spatial proximity corresponds to expression pattern similarity. Each nanobiopsy transcriptome was visualized as a component of SOM (Fig. 2*D*; four representative nanobiopsy components shown for each cellular compartment type).

Nanobiopsy is an unbiased and sensitive way of neurite transcriptome sampling

Nanobiopsy can sample repeatedly from cell bodies and neurites of the same cell, and because we can collect sample from a very small subcellular area, the transcript sets do not need to undergo any data filtering. To examine the sensitivity of nanobiopsy sampling, we compared the mRNA repertoire in our nanobiopsy samples to all genes detected in axon or dendrite by bulk microarray analysis, RNA sequencing, and *in situ* hybridization in previous studies (3–7, 16, 18, 19, 24–41) (Fig. 3*A* and Table S5). Sampling from 30 neurites enabled the identification of 929 transcripts that localize to neuronal processes. Although the total number of genes was smaller compared with bulk sampling, we found 178 transcripts in neurites that were not detected in previous studies (Fig. 3*A*). When performing bulk sampling, the relative number of rare transcripts is very low, partly because the fragments can be lost during purification steps, and their sequencing read signal intensities may be regarded as noise. Our nanobiopsy platform can collect a miniscule amount of cytosolic material, and a rare transcript could be present in a relatively higher amount in a smaller sample. Nanobiopsy samples are directly reverse transcribed, and the cDNA is amplified, without cell lysis or RNA purification steps, thus further reducing the loss of rare transcripts.

The new discovered transcripts localizing to neurites belong to various functional categories, such as neuron development, immune system, cell signaling, and even proteins annotated as nuclear. Some of the new genes we found encode proteins involved in immune response. Our highly sensitive nanobiopsy sampling of neuronal cells has shown for the first time that the mRNAs encoding the Toll-like receptor 5 (*Tlr5*) are part of the mRNA repertoire of neurites. We were surprised to see that many of the new transcripts we sampled from neuronal processes encode proteins that function in the nucleus. This includes transcription factors, which are important in nervous system development, such as EOMES. Nanobiopsy sampling has also shown that mRNAs encoding many histone-remodeling enzymes are transported to neurites as well, such as the lysine demethylase *Kdm5c* and general constituents of the DNA replication or the transcription machinery such as the double-stranded DNA unwinding protein HMGB3, the mini-chromosome maintenance binding protein MCMBP, and the transcription elongation factor TCEAL7. There is very little known about the function of nuclear proteins that are synthesized or transported to the peripheral areas of neurons. Our report is the first to show that transcripts encoding DNA-unwinding or histone remodeling proteins are part of the mRNA repertoire of neurites.

To verify the localization of these transcripts in neurites, we performed fluorescent *in situ* hybridization on a chosen set of genes (Fig. 3*C*). We selected a diverse set of genes for the validation experiment, including genes encoding nuclear proteins, a component of the translation machinery, a protein that has differential expression in brain, and a component of mitochondrial inner membrane. We put more emphasis on nuclear genes because their localization to neurites is less understood. All of the mRNAs for which we developed probes were detected in the neurites. Control experiments lacking the initial probe showed no fluorescent signal. The experiment has shown that these mRNAs are localized to neurites in only ~10–15% of the neurons and that they are present in neurites in a very low amount as shown by the low number of fluorescent spots. Some RNAs with low copy numbers in neurites included genes that encode nuclear genes such as the double-stranded DNA unwinding protein HMGB3, the mini-chromosome maintenance binding protein MCMBP, and the transcription elongation factor TCEAL7 (Fig. 3*C*). Some of the non-nuclear genes we detected were brain-expressed X-linked 5, eukaryotic translation initiation factor 2, subunit 3, and apolipoprotein A (Fig. 3*C*). Thus, fluorescent *in situ* hybridization confirmed that nanobiopsy is a sensitive and reliable method for the detection of low abundance transcripts in neuronal extensions.

The cell body is a transport hub of neuronal mRNA and protein compartmentalization

We next compared the list of genes we identified in our cell body and neurite nanobiopsy samples (Fig. 3*B* and Table S6). The two gene sets showed little overlap (~200 genes), demonstrating the functional difference between the two subcellular compartments.

To get a general overview of the repertoire of mRNAs that localize to neuronal cell bodies, we analyzed the pooled expression data from all cell body nanobiopsy samples (13 samples, 1292 genes) (Table 1, Table S7, and Fig. S2). This gene set was significantly enriched for the Gene Ontology (GO) terms "cel-

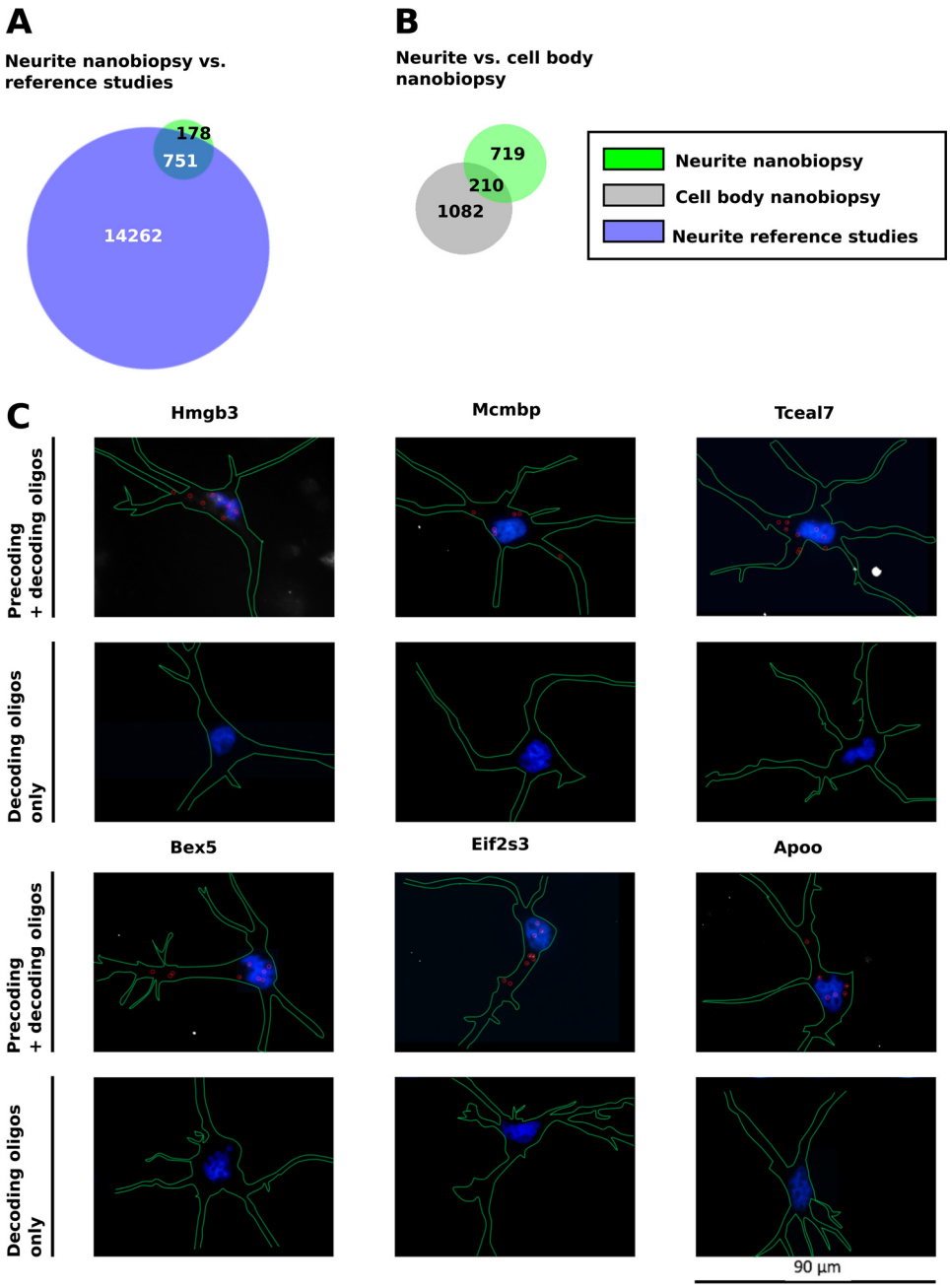

Figure 3. Nanobiopsy sampling/RNA-seq is able to collect and identify rare transcripts that are not detected via bulk sampling methods. *A*, Venn diagram of the genes detected by neurite nanobiopsy, and the genes identified in axon and dendrite by previous bulk microarray, RNA-seq or *in situ* hybridization studies (3–7, 16, 18, 19, 24–41). *B*, Venn diagram of the genes detected by cell body and neurite nanobiopsy of neuronal cells. All Venn diagrams are area-proportional; the *labels* indicate the number of genes. *C*, validation of nanobiopsy sampling and RNA-seq by high-resolution fluorescent *in situ* hybridization. The cells were first treated with a set of unlabeled predecoding oligonucleotides binding the target gene and subsequently hybridized with fluorescently labeled decoding oligonucleotides. Transcripts validated include *Hmgb3*, *Mcmbp*, *Tceal7*, *Bex5*, *Eif2s3*, and *Apoo*. *White spots* encircled with *red* indicate fluorescent spots corresponding to the target mRNA. *Blue* indicates 4′,6′-diamino-2-phenylindole–stained nuclei.

Table 1

Gene Ontology Enrichment analysis of all transcripts identified in all nanobiopsy samples taken from cell bodies and neurites of human induced pluripotent stem cell–derived neuronal cells

Cell body	*p* value	Neurite	*p* value
Cellular localization	2.23E-26	Translation initiation	3.83E-15
Intracellular transport	9.66E-22	Nuclear transcribed mRNA catabolic process, nonsense-mediated decay	5.66E-14
Cellular protein localization	1.17E-20	Establishment of protein localization to endoplasmic reticulum	7.52E-14
Translational initiation	3.97E-14	Cellular localization	2.32E-11
Cellular component biogenesis	2.34E-13	Cellular component biogenesis	2.34E-11
Cytoskeleton organization	2.64E-11	mRNA metabolic process	4.96E-11
RNA processing	1.76E-11		

Table 2
Gene Ontology Enrichment analysis of all transcripts that had at least four reads mapped to the human genome in cell body nanobiopsy samples taken from human iPS-derived neuronal cells

Cell body	*p* value
Neuron projection development	4.25E-7
Nervous system development	1.78E-6
Microtubule-based process	1.08E-5
Neuron differentiation	1.58E-5

lular localization" (*p* value, 2.23E-26), "intracellular transport" (*p* value, 9.66E-22), and "cellular protein localization" (*p* value, 1.17E-20). 301, 206, and 274 genes were annotated to these three GO terms. These included mRNA encoding the microtubule tethering protein HOOK, the anchoring protein AKAP12 that regulates the subcellular compartmentation of protein kinase A (42), the $GABA_A$ receptor-associated protein (GABARAP), as well as the RNA-binding protein RANBP1. The GO term "cellular component biogenesis" was also significantly enriched (*p* value, 2.34E-13). 288 genes were annotated to this term; the majority of them are cytoskeletal or nuclear proteins, including components of the microtubule cytoskeleton or chromatin. Additionally, cell-body transcripts exhibited strong up-regulation of genes involved in translational initiation (*p* value, 3.97E-14) and RNA processing (*p* value, 1.76E-11).

When we looked at the genes that can be considered a higher expression level caused by having at least four reads mapped uniquely to an annotated transcript (259 genes), "neuron projection development" (*p* value, 4.25E-7) was the most highly enriched GO term, followed by "microtubule-based process" (*p* value, 1.08E-5) (Table 2, Table S7, and Fig. S3). Genes involved in neuronal projections development include *Rtn4* (43), a developmental neurite growth regulatory factor, and *Stmn2*, which controls neurite length in neuronal cells (44). Taken together, our data suggest that the neuron cell body is mainly involved in regulating gene expression, synthesizing mRNA and proteins, transporting and redistributing them to the neurites, and creating a complex, modular, fine-tunable supply network for axon and dendrites.

The neurite mRNA repertoire is enriched in transcripts related to mRNA processing, protein synthesis, and transport

To get a general comparison of the mRNA profile of the neuronal processes, we examined the pooled expression data from all neurite nanobiopsy samples (30 samples, ~930 genes) (Table 1, Table S7, and Fig. S4). We found that neurite transcripts are highly enriched for GO categories related to protein synthesis, such as "translational initiation" (*p* value, 3.83E-15). 40 genes were annotated to this GO term, including genes encoding ribosomal proteins. Neuronal processes also showed enrichment for the GO term "mRNA metabolic process" (*p* value, 4.96E-11). 73 genes mapped to this GO term, including the mRNA splicing gene *Ddx5*. Furthermore, neurites showed enrichment for the Gene Ontology terms "establishment of protein localization to endoplasmic reticulum" (*p* value, 7.52E-14) and "cellular localization" (*p* value, 2.32E-11). 29 and 190 genes mapped to these GO terms, including genes involved in microtubule-mediated transport or protein targeting to ER.

mRNA shows a mosaic pattern of localization in neuronal cells

To get a deeper insight into the spatial dynamics of mRNA compartmentalization and distribution in neuronal cells, we analyzed single-nanobiopsy components of the SOM (Fig. 4). Because the amount of cytosolic material collected during each biopsy sampling is only ~1% of the cell's total volume, we could compare very small segments of the cellular space to each other. Nanobiopsy samples showed great variability in terms of the number (Fig. 2, *A* and *B*) and the identity of transcripts (Fig. 4) they contained. This indicated that the cellular mRNA pool cannot be considered well-mixed and homogeneous and that subcellular areas fundamentally differ from each other in terms of their mRNA composition. The two most commonly found gene clusters (Cluster 1 and Cluster 2) (Table S8) did not show any significant enrichment for any Gene Ontology term. These clusters included genes such as the large ribosomal subunit protein *Rpl8*, the DNA-unwinding protein *Hmgb3*, the mitochondrial import inner membrane translocase subunit *Timm10*, or the E3 ubiquitin ligase complex substrate adapter protein *Keap1*.

mRNAs encoding functionally related proteins often localize to the same subcellular place

To dissect the functional significance of the elaborate mRNA compartmentalization pattern in neuronal cells, we examined the gene clusters that showed similar expression patterns across samples (Fig. 4 and Table S8). Most gene clusters contained functionally unrelated transcripts. However, we were surprised to see that a subset of the gene clusters was enriched for a common GO term (Table S9). Cluster 4, found in one cell body nanobiopsy sample, was significantly enriched for the GO term "intracellular transport" (*p* value, 4.29E-11). 120 genes were annotated to this GO term, including the kinesin-like protein *Kif13a* or the protein transport gene *Sec24d*. Cluster 3, another cell body nanobiopsy sample, showed enrichment for the GO term "protein dephosphorylation" (*p* value, 1.31E-3). Seven protein phosphatases mapped to this GO term, including *Ptprb* and *Dusp1*. Cluster 7, found in one of the neurite nanobiopsy samples, showed enrichment for the GO term "respiratory electron transport chain" (*p* value, 4.44E-7). Five mitochondrial genes were annotated to this term, including NADH-dehydrogenase subunits and cytochrome *c*-oxidase subunits. Cluster 14, found in another one of the neurite nanobiopsy samples, showed significant enrichment for the GO term "translational initiation" (*p* value, 7.60E-6). Nine genes were annotated to this GO term, including the ribosomal proteins *Rpl39*, *Rpl10*, *Rpl11*, and *Rpl*l7. Overall, these results suggest that neuronal cells take advantage of sophisticated mRNA-transport mechanisms to establish defined mRNA compartmentalization patterns to fine-tune the molecular functions of the subcellular segments in response to extracellular stimuli.

Discussion

Neurons are highly polarized cells that take great advantage of compartmentalizing mRNA and locally translating it wherever and whenever it is needed (1). To examine the pattern of mRNA compartmentalization in neuronal cells, we extracted miniscule cytosolic samples from cell bodies and neurites using

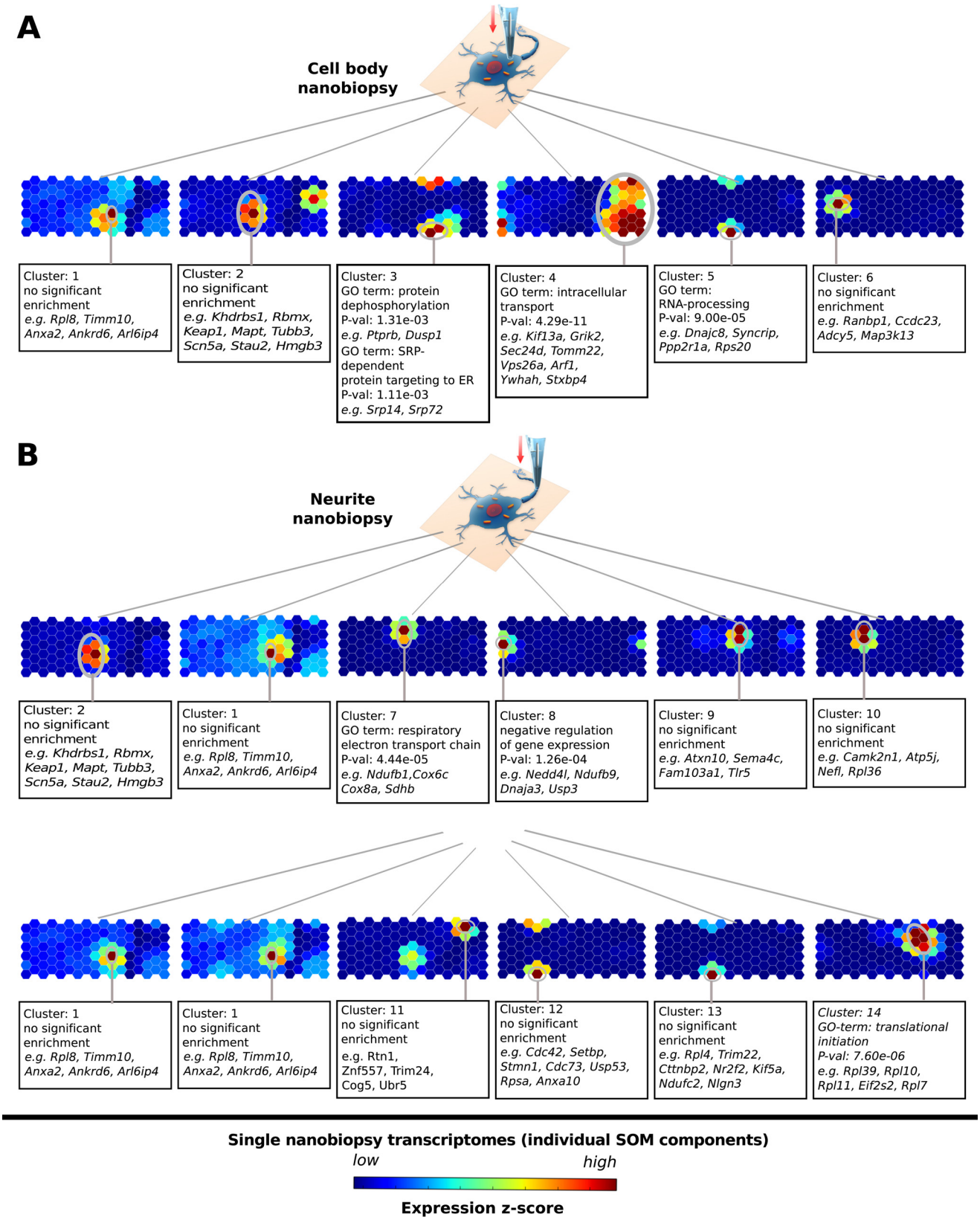

Figure 4. Analysis of mRNA compartmentalization pattern in neuronal cells by nanobiopsy sampling and RNA-seq analysis using the self-organizing map. The self-organizing map consists of units representing a group of genes whose expression patterns across samples are most similar. The units are clustered and have fixed positions across all nanobiopsy components of the SOM. Individual nanobiopsy transcriptomes can be plotted by mapping the genes expressed in the sample onto the SOM. Gene clusters are defined as groups of units that are next to each other and are often co-expressed in cells. Above, representative single-nanobiopsy transcriptomes depicted as individual components of the SOM are shown. *Boxes* represent individual nanobiopsy samples taken from neuronal cell bodies (*A*) or neurites (*B*). Gene clusters are outlined in *gray*.

our label-free, single-cell nanobiopsy platform, prepared the cDNA, and performed next generation RNA sequencing. Our easy-to-operate, flexible platform allowed us to sample from any subcellular compartment of neural cells with high spatial resolution and precision. We collected 43 nanobiopsy samples in total and identified more than 2000 transcripts.

Our analysis has shown that the repertoire of mRNAs that localized to cell bodies is highly enriched for genes related to intracellular transport including genes regulating cytoskeleton organization, protein and RNA-transport, vesicle trafficking, and transcription activation. This indicates the importance of distributing the mRNA and protein to the peripheral sites of the neuronal cell through highly regulated and sophisticated transport mechanisms.

The neurite transcriptome was highly enriched for genes related to protein synthesis, protein targeting to ER, ribosome biogenesis, and RNA metabolism. It has been reported before that neuronal growth cones respond to attractive (brain-derived neurotrophic factor, netrin) and repulsive (SEM3A, SLIT2B) guidance cues by regulating the local translation of the cytoskeletal protein β-actin and the actin cytoskeleton remodeling proteins cofilin and RhoA (11, 45, 46). Newly synthesized β-actin has higher polymerization ability compared with old, covalently modified β-actin. Thus, it significantly affects growth cone dynamics (47). Neurotrophic factors also induce the axonal translation of Bclw that prevents axonal degeneration and promotes axon maintenance (12). Following neuron injury, local translation is required for neurite regeneration (13). Taken together, regulating local translation of mRNA and regulation of protein levels is one of the major ways that neurites respond to extracellular stimuli and maintain a physiologically accurate composition.

Our highly sensitive nanobiopsy sampling approach enabled the detection in neurites of ~200 very low expression level transcripts that could not be found by using previously employed bulk sampling methods. To our great surprise, many of these transcripts encode nuclear proteins, such as the transcription factor EOMES, the double-stranded DNA unwinding protein HMGB3, the mini-chromosome maintenance binding protein MCMBP, and the transcription elongation factor TCEAL7.

Although unexpected, there is a growing body of evidence indicating the presence of transcripts encoding nuclear proteins in axons and dendrites. Nuclear genes can have additional functions, unrelated to nucleus. The nuclear scaffolding protein Lamin B2 is translated in axons, where it binds mitochondria, and is required for the maintenance of axonal integrity (48). Some transcription factors (*e.g.* CREB and SMAD 1/5/8) are translated in axons following neurotrophic factor stimulation or injury, retrogradely transported to nucleus, and act as transcription factors to promote neuron survival (49, 50). Up to now there was only limited evidence showing the importance of the dendritic synthesis of transcription factors in the dendrite-soma signaling (51, 52). Ainsley *et al.* (6) have shown that H4 histone and Mediator complex member mRNAs are localized to dendrites. Thus, transcription factors synthesized in the periphery and interacting with the local signaling environment may carry some unique information or function, allow a local response, and contribute to the synapse–axon–nucleus signaling axis. In addition, the time delay required for these transcription factors to be translated in the axon and retrogradely transported to the nucleus may be an essential part of the temporal dynamics of neuronal cell physiology. Alternatively, the signal for transport to the nucleus may depend upon other environmental cues encountered at the periphery. Thus, our study can help establish the comprehensive list of nuclear genes that localize to neurites and help us shed light on the possible function of these genes.

We have also definitively shown that the neuronal mRNA pool cannot be considered well-mixed and homogeneous, in that subcellular areas fundamentally differ from each other in terms of their mRNA composition. This is in agreement with a previous study showing that in *Drosophila* embryos, >70% of the mRNA transcripts analyzed appeared to be regionally distributed (53). Nanobiopsy samples showed great variability in the number and the kind of transcripts they contained. Analyzing gene clusters that showed similar expression pattern across samples we found that some gene clusters showed functional enrichment. For example, mRNAs encoding genes related to cytoskeleton remodeling or protein translation localized to the same subcellular space. Recent reports have shown the presence of translationally active hot spots in cells (54–56) and that in primary neurons, mRNAs display "bursting" translation (57). Translation machinery components are often anchored to the plasma membrane and are being released upon activation of transmembrane receptors and initiation of local signaling, enabling local translation of mRNA (58). Furthermore, proteins synthesized at distal sites are more likely to be rich in assembly-promoting domains and are often regulated by post-translational modification sites (59). Thus, compartmentalizing mRNAs encoding proteins of related function to the same subcellular area can contribute to the coordinated, local synthesis of these proteins, and the formation of cellular multiprotein assemblies in response to extracellular stimuli. Some sequence motifs located in the 3′-UTR, 5′-UTR, intron, or coding sequence of an mRNA, as well as RNA-binding proteins regulating the transport of mRNAs to neuronal processes, have been identified (9, 60, 61). However, the mechanisms by which most of the several thousand mRNAs that localize to neuronal axons and dendrites are transported are still unknown.

Our nanobiopsy sampling and analysis revealed that neuronal cells take advantage of sophisticated mRNA-localization mechanisms to establish defined mRNA compartmentalization patterns. This allows neuronal cells to fine-tune the molecular functions of the subcellular segments according to an endogenous program, as well as in response to extracellular stimuli. This technique could be of use for further probing of the subcellular localization of mRNA in various polarized cells.

Experimental procedures

Neuronal cell culture

The neuronal cells cultured for this study were hiPSC-derived neurons (iCell neurons) obtained from Cellular Dynamics International (Madison, WI). The cryopreserved cells were a more than 95% pure population consisting of GABAergic and

glutamatergic neurons, with less than 1% of dopaminergic neurons (information provided by CDI, Madison, WI). For nanobiopsy experiments, the cells were plated at 20,000 cells/cm^2 density in 3.5-cm diameter, CELLview^{TM} cell culture dishes (Greiner Bio-One GmbH, Rainbach im Mühlkreis, Austria) pretreated with 0.05% polyethyleneimine (Sigma–Aldrich) for 1 h and coated with 5.0 μg/ml laminin (Sigma–Aldrich) for 1 h. For fluorescent *in situ* hybridization experiments, iCell GABANeuron cells (new catalogue name for iCell Neurons) were plated at 10,000 cells/well on eight-well chambered coverglass (Thermo Scientific), which were precoated with 0.01% poly-L-ornithine (Sigma–Aldrich) for 1 h and 5.0 μg/ml laminin (Sigma–Aldrich) solution for 1 h.

The cells were grown in medium provided by Cellular Dynamics supplemented with 1% PenStrep (Lonza, Basel, Switzerland) at 37 °C, with 5% CO_2, 95% air. To better visualize cell morphology for nanobiopsy, the cells were transfected with pEGFP-c1-Tau (Kan resistance) plasmid using GeneJuice® transfection reagent (Merck Millipore, Billerica, MA), according to the manufacturer's instructions. The plasmid was a generous gift of Steve Finkbeiner's laboratory from the Gladstone Institute at University of California, San Francisco.

Electrowetting in nanopipettes

Nanopipettes were fabricated as previously described (20). Briefly, nanopipettes with a mean diameter of 106 ± 16 nm were made from quartz capillaries (Sutter Instrument, Novato, CA) using a P-2000 laser puller (Sutter Instrument). Quartz capillaries were filled with a 10 nM tetrahexylammonium tetrakis-(4-chlorophenyl)borate (THATPBCI) solution in 1,2-dichloroethane (DCE). An Ag/AgCl wire was then inserted into the barrel of the nanopipette, whereas an Ag/AgCl wire was submerged in the medium of the cell culture acting as a reference/counter electrode.

SICM setup

The scanning ion conductance microscope was set up as described previously (20). The SICM consisted of an Axopatch 200B low-noise amplifier (Molecular Devices, Sunnyvale, CA) for nanopipette bias and current measurement. The nanopipette was spatially manipulated with an MP-285 micromanipulator (Sutter Instrument) for coarse control and a Nano-piezo actuator (Physik Instrumente, Irvine, CA) for fine control. A PCIe-7851R field-programmable gate array (National Instruments) was used for hardware control of the system. A custom-coded software written in LabVIEW (National Instruments) was used to operate the system, enabling cell surface finding, penetration, and collection of cellular material automatically. The volume of aspirated cellular material was ~50 fl, which corresponded to ~1% of the total volume of an average cell.

RNA-seq, cDNA synthesis, and sequencing

cDNA was synthesized from aspirated RNA samples using the ultra low RNA input SMART-Seq system (Takara Bio USA, Mountain View, CA). The cDNA was prepared for each individual aspiration for library preparation. All 43 nanobiopsy samples and 1 negative control sample were supplemented with 0.5 μl of 1:5000 diluted ERCC Spike-In Mix 1 (Ambion) for quality control and sensitivity check. cDNA was amplified by a KAPA HiFi HotStart ReadyMix PCR kit (KAPA Biosystems, Wilmington, MA), using SMART-Seq PCR primers. cDNA was purified by AmPure XP beads (Beckman Coulter Genomics, Danvers, MA). The quality and quantity of single-cell cDNA was evaluated using the Agilent Bioanalyzer 2100 high sensitivity DNA assay (Agilent, Palo Alto, CA).

Tagmentation of cDNA for the preparation of RNA-seq libraries was performed by Nextera XT DNA library preparation kit (Illumina, San Diego, CA). Multiplexed sequencing adapters were ligated to tagmented cDNA by limited-cycle PCR (10 cycles), according to the manufacturer's instructions. The final, amplified libraries were purified by AmPure XP beads (Beckman Coulter Genomics, Danvers, MA), and size-selected in the range of 200–600 bp using the Caliper LabChip XT system (PerkinElmer). The final RNA-seq libraries were quantified using the Agilent Bioanalyzer 2100 high sensitivity DNA assay and KAPA library quantification kit and pooled together in equal concentration for sequencing. The pooled multiplexed libraries were sequenced for 2 × 150 bp paired-end or 2 × 80 bp paired-end reads on Illumina MiSeq (Illumina, San Diego, CA).

RNA sequencing read mapping

RNA-seq reads were aligned to the hg38 UCSC human reference genome using STAR aligner (62). Genes were scored positive for expression if at least one read mapped uniquely to an annotated transcript. Gene expression was quantified using HTSeq (63). Venn diagrams were created by the BioVenn web application (64).

Gene Ontology Enrichment Analysis

Gene Ontology Enrichment Analysis was performed using the DAVID Functional Annotation tool (65). Relevant GO terms were visualized as tree maps using the REVIGO server (66).

Self-organizing maps

SOM were constructed as described (23). Before constructing the Self-Organizing Map, each gene expression value was normalized on a gene-by-gene basis by subtracting each gene expression mean and dividing by its standard deviation across libraries. A self-organizing map was trained with the 1,000 genes of the highest variance among the nanobiopsy samples, using the R package Kohonen (67). The total number of map units was set to the heuristic value 3*sqrt(N), where N corresponds to the number of genes used for the training. Initial values were assigned to the grid by multiplying the first two principal components of the data by a sinusoidal function and the training lasted 200 epochs. Clusters were seeded by the local minima of the u-matrix, with a value for each unit defined as the average of the vector difference between that unit's prototype and its six neighbors on the hexagonal grid. All other unit prototypes were then assigned to clusters according to the minimum vector distance to a seed unit. All expressed genes were mapped onto the SOM, and visualized using a custom Python code. The lists of clustered genes were submitted to the DAVID Functional Annotation tool (65) to determine enriched terms.

Synthesis of decoding fluorescent oligonucleotides

Quasar 570 labeled oligonucleotide probes were prepared according to the previously described method (22). Briefly, 1 nmol of 5′-amino-modified oligonucleotides (Integrated DNA Technologies, Coralville, IA) were dissolved in 3 μl of nuclease-free 1× PBS buffer (pH 7.4). To this solution, 3 μl of sodium tetraborate (1 M, pH 8.5) in anhydrous dimethylformamide were added. The reaction mixture was incubated at room temperature for at least 3 h. Subsequently, fluorophore-coupled oligonucleotides were purified by nucleotide removal kit (Qiagen) and then further purified via a HPLC equipped with C18 column (Agilent). The purified product was dried completely in SpeedVac, subsequently dissolved in 200 μl of nuclease-free 1× PBS (pH 7.4), and stored at 4 °C as a stock solution.

In situ RNA labeling

Cultured iCell GABANeurons were first washed with nuclease-free 1× PBS for 5 min at room temperature and then fixed with fixation solution (4% formaldehyde (Polysciences) in 1× PBS) at room temperature for 20 min. Subsequently, the cells were washed twice with 1× PBS at room temperature, each for 5 min. Finally, fixed cells were permeabilized with 70% ethanol for overnight at 4 °C.

Unlabeled predecoding oligonucleotides belonging to one library (each with a 25 pmol) were dissolved in 100 μl of nuclease-free 1× PBS (pH 7.4) to obtain a stock solution. To 100 μl of predecoding hybridization buffer (100 mg/ml dextran sulfate, 20 μg/ml bovine serum albumin, 1 mg/ml *Escherichia coli* tRNA, 2 mM vanadyl ribonucleoside complex, and 10% formamide in 2× saline-sodium citrate (SSC)), 1 μl of stock unlabeled probe library was added to obtain predecoding hybridization solution. Fixed iCell GABANeurons were first washed with wash buffer (10% formamide in 2× SSC, 2 mM vanadyl ribonucleoside complex) for 5 min at room temperature. Then cells were incubated with the predecoding hybridization solution at 37 °C for overnight. Next day, the cells were washed with wash buffer twice at 37 °C for 30 min.

To 100 μl of decoding hybridization buffer (10% formamide in 2× SSC, 100 mg/ml of dextran sulfate, and 2 mM vanadyl ribonucleoside complex), 5 μl of Quasar 570 labeled stock probe solution was added to obtain decoding hybridization solution. Then cells were incubated with decoding hybridization solution at 37 °C for 30 min and subsequently washed with wash buffer at 37 °C for 30 min once. The stained cells were first equilibrated with freshly prepared GLOX buffer (0.4% glucose, 10 mM Tris-HCl in 2× SSC) and subsequently imaged in GLOX solution (1% catalase, 0.37 mg/ml glucose oxidase, 0.4% glucose, and 10 mM Tris-HCl in 2× SSC).

Fluorescent in situ hybridization imaging and data processing

The stained cells were imaged under a Nikon Ti-E epifluorescence microscope equipped with 100× objective, using a 5-μm z range and 0.3-μm z spacing. All images were captured by CoolSNAP HQ2 camera and analyzed with NIS-Elements imaging software. Chroma filter 49004 was used to image Quasar 570 channel. All z images were stacked and aligned using ImageJ software.

Author contributions—N. P. conceived the study, designed and supervised all aspects of the study and edited the manuscript; E. N. T. designed experiments, collected nanobiopsy samples, prepared sequencing libraries, performed sequencing, analyzed data, and wrote the manuscript; A. L. contributed to preparing sequencing libraries, performing sequencing, and editing the manuscript; A. F. supervised the study and contributed to experimental design and editing the manuscript; and J. G. and M. M. performed fluorescent *in situ* hybridization experiments.

Acknowledgments—We acknowledge Gepoliano Chaves and Thomas Boser (University of California at Santa Cruz) for bioinformatics analysis. We thank Shirley Pepke and Daniel Kim (California Institute of Technology and University of California at Santa Cruz, respectively) for expert advice on constructing self-organizing maps. We also thank Kazue Okubo (Genostaff, Tokyo, Japan), Kenzo Bamba (University of Tsukuba, Tsukuba, Japan), Yasu-Yuki Kida, Yuzo Takayama (National Institute of Advanced Industrial Science and Technology, Tsukuba, Japan), and Misuzu Hashimoto (University of Tsukuba, Tsukuba, Japan) for helpful discussions.

References

1. Jung, H., Gkogkas, C. G., Sonenberg, N., and Holt, C. E. (2014) Remote control of gene function by local translation. *Cell* **157,** 26–40 CrossRef Medline
2. Schwanhäusser, B., Busse, D., Li, N., Dittmar, G., Schuchhardt, J., Wolf, J., Chen, W., and Selbach, M. (2011) Global quantification of mammalian gene expression control. *Nature* **473,** 337–342 CrossRef Medline
3. Gumy, L. F., Yeo, G. S., Tung, Y.-C. L., Zivraj, K. H., Willis, D., Coppola, G., Lam, B. Y., Twiss, J. L., Holt, C. E., and Fawcett, J. W. (2011) Transcriptome analysis of embryonic and adult sensory axons reveals changes in mRNA repertoire localization. *RNA* **17,** 85–98 CrossRef Medline
4. Minis, A., Dahary, D., Manor, O., Leshkowitz, D., Pilpel, Y., and Yaron, A. (2014) Subcellular transcriptomics-dissection of the mRNA composition in the axonal compartment of sensory neurons. *Dev. Neurobiol.* **74,** 365–381 CrossRef Medline
5. Cajigas, I. J., Tushev, G., Will, T. J., tom Dieck, S., Fuerst, N., and Schuman, E. M. (2012) The local transcriptome in the synaptic neuropil revealed by deep sequencing and high-resolution imaging. *Neuron* **74,** 453–466 CrossRef Medline
6. Ainsley, J. A., Drane, L., Jacobs, J., Kittelberger, K. A., and Reijmers, L. G. (2014) Functionally diverse dendritic mRNAs rapidly associate with ribosomes following a novel experience. *Nat. Commun.* **5,** 4510–4520 Medline
7. Shigeoka, T., Jung, H., Jung, J., Turner-Bridger, B., Ohk, J., Lin, J. Q., Amieux, P. S., and Holt, C. E. (2016) Dynamic axonal translation in developing and mature visual circuits. *Cell* **166,** 181–192 CrossRef Medline
8. Buckley, P. T., Lee, M. T., Sul, J. Y., Miyashiro, K. Y., Bell, T. J., Fisher, S. A., Kim, J., and Eberwine, J. (2011) Cytoplasmic intron sequence-retaining transcripts (CIRTs) can be dendritically targeted via ID element retrotransposons. *Neuron* **69,** 877–884 CrossRef Medline
9. Jung, H., Yoon, B. C., and Holt, C. E. (2012) Axonal mRNA localization and local protein synthesis in nervous system assembly, maintenance and repair. *Nat. Rev. Neurosci.* **13,** 308–324 CrossRef Medline
10. Leung, K.-M., van Horck, F. P., Lin, A. C., Allison, R., Standart, N., and Holt, C. E. (2006) Asymmetrical β-actin mRNA translation in growth cones mediates attractive turning to netrin-1. *Nat. Neurosci.* **9,** 1247–1256 CrossRef Medline
11. Yao, J., Sasaki, Y., Wen, Z., Bassell, G. J., and Zheng, J. Q. (2006) An essential role for β-actin mRNA localization and translation in Ca^{2+}-dependent growth cone guidance. *Nat. Neurosci.* **9,** 1265–1273 CrossRef Medline
12. Cosker, K. E., Pazyra-Murphy, M. F., Fenstermacher, S. J., and Segal, R. A. (2013) Target-derived neurotrophins coordinate transcription and trans-

port of Bclw to prevent axonal degeneration. *J. Neurosci.* **33,** 5195–5207 CrossRef Medline
13. Verma, P., Chierzi, S., Codd, A. M., Campbell, D. S., Meyer, R. L., Holt, C. E., and Fawcett, J. W. (2005) Axonal protein synthesis and degradation are necessary for efficient growth cone regeneration. *J. Neurosci.* **25,** 331–342 CrossRef Medline
14. Doyle, M., and Kiebler, M. (2011) a Mechanisms of dendritic mRNA transport and its role in synaptic tagging. *EMBO J.* **30,** 3540–3552 CrossRef Medline
15. Ramaswami, M., Taylor, J. P., and Parker, R. (2013) Altered ribostasis: RNA-protein granules in degenerative disorders. *Cell* **154,** 727–736 CrossRef Medline
16. Zivraj, K. H., Tung, Y. C., Piper, M., Gumy, L., Fawcett, J. W., Yeo, G. S., and Holt, C. E. (2010) Subcellular profiling reveals distinct and developmentally regulated repertoire of growth cone mRNAs. *J. Neurosci.* **30,** 15464–15478 CrossRef Medline
17. Poon, M. M., Choi, S.-H., Jamieson C. A., Geschwind, D. H., and Martin, K. C. (2006) Identification of process-localized mRNAs from cultured rodent hippocampal neurons. *J. Neurosci.* **26,** 13390–13399 CrossRef Medline
18. Francis, C., Natarajan, S., Lee, M. T., Khaladkar, M., Buckley, P. T., Sul, J.-Y., Eberwine, J., and Kim, J. (2014) Divergence of RNA localization between rat and mouse neurons reveals the potential for rapid brain evolution. *BMC Genomics* **15,** 883 CrossRef Medline
19. Crino, P. B., and Eberwine, J. (1996) Molecular characterization of the dendritic growth cone: regulated mRNA transport and local protein synthesis. *Neuron* **17,** 1173–1187 CrossRef Medline
20. Actis, P., Maalouf, M. M., Kim, H. J., Lohith, A., Vilozny, B., Seger, R. A., and Pourmand, N. (2014) Compartmental genomics in living cells revealed by single-cell nanobiopsy. *ACS Nano.* **8,** 546–553 CrossRef Medline
21. Jiang, L., Schlesinger, F., Davis C. A., Zhang, Y., Li, R., Salit, M., Gingeras, T. R., and Oliver, B. (2011) Synthetic spike-in standards for RNA-seq experiments. *Genome Res.* **21,** 1543–1551 CrossRef Medline
22. Xiao, L., and Guo, J. (2015) Multiplexed single-cell in situ RNA analysis by reiterative hybridization. *Anal. Methods* **7,** 7290–7295 CrossRef
23. Kim, D. H., Marinov, G. K., Pepke, S., Singer, Z. S., He, P., Williams, B., Schroth, G. P., Elowitz, M. B., and Wold, B. J. (2015) Single-cell transcriptome analysis reveals dynamic changes in lncRNA expression during reprogramming. *Cell Stem Cell* **16,** 88–101 CrossRef Medline
24. Andreassi, C., and Riccio, A. (2009) To localize or not to localize: mRNA fate is in 3′UTR ends. *Trends Cell Biol.* **19,** 465–474 CrossRef Medline
25. Aschrafi, A., Natera-Naranjo, O., Gioio, A. E., and Kaplan, B. B. (2010) Regulation of axonal trafficking of cytochrome c oxidase IV mRNA. *Mol. Cell. Neurosci.* **43,** 422–430 CrossRef Medline
26. Brittis, P. A., Lu, Q., and Flanagan, J. G. (2002) Axonal protein synthesis provides a mechanism for localized regulation at an intermediate target. *Cell* **110,** 223–235 CrossRef Medline
27. Hengst, U., Deglincerti, A., Kim, H. J., Jeon, N. L., and Jaffrey, S. R. (2009) Axonal elongation triggered by stimulus-induced local translation of a polarity complex protein. *Nat. Cell Biol.* **11,** 1024–1030 CrossRef Medline
28. Jirikowski, G. F., Sanna, P. P., and Bloom, F. E. (1990) mRNA coding for oxytocin is present in axons of the hypothalamo-neurohypophysial tract. *Proc. Natl. Acad. Sci. U.S.A.* **87,** 7400–7404 CrossRef Medline
29. Kuwako, K., Kakumoto, K., Imai, T., Igarashi, M., Hamakubo, T., Sakakibara, S., Tessier-Lavigne, M., Okano, H. J., and Okano, H. (2010) Neural RNA-binding protein Musashi1 controls midline crossing of precerebellar neurons through posttranscriptional regulation of Robo3/Rig-1 expression. *Neuron* **67,** 407–421 CrossRef Medline
30. Merianda, T. T., Lin, A. C., Lam, J. S., Vuppalanchi, D., Willis, D. E., Karin, N., Holt, C. E., and Twiss, J. L. (2009) A functional equivalent of endoplasmic reticulum and Golgi in axons for secretion of locally synthesized proteins. *Mol. Cell. Neurosci.* **40,** 128–142 CrossRef Medline
31. Moccia, R., Chen, D., Lyles, V., Kapuya, E., E, Y., Kalachikov, S., Spahn, C. M., Frank, J., Kandel, E. R., Barad, M., and Martin, K. C. (2003) An unbiased cDNA library prepared from isolated Aplysia sensory neuron processes is enriched for cytoskeletal and translational mRNAs. *J. Neurosci.* **23,** 9409–9417 Medline
32. Pfeiffer-Guglielmi, B., Dombert, B., Jablonka, S., Hausherr, V., van Thriel, C., Schöbel, N., and Jansen, R.-P. (2014) Axonal and dendritic localization of mRNAs for glycogen-metabolizing enzymes in cultured rodent neurons. *BMC Neurosci.* **15,** 70–81 CrossRef Medline
33. Taylor, A. M., Berchtold, N. C., Perreau, V. M., Tu, C. H., Li Jeon, N., and Cotman, C. W. (2009) Axonal mRNA in uninjured and regenerating cortical mammalian axons. *J. Neurosci.* **29,** 4697–4707 CrossRef Medline
34. Willis, D. E., van Niekerk, E. A., Sasaki, Y., Mesngon, M., Merianda, T. T., Williams, G. G., Kendall, M., Smith, D. S., Bassell, G. J., and Twiss, J. L. (2007) Extracellular stimuli specifically regulate localized levels of individual neuronal mRNAs. *J. Cell Biol.* **178,** 965–980 CrossRef Medline
35. Bramham, C. R., and Wells, D. G. (2007) Dendritic mRNA: transport, translation and function. *Nat. Rev. Neurosci.* **8,** 776–789 CrossRef Medline
36. Eberwine, J., Belt, B., Kacharmina, J. E., and Miyashiro, K. (2002) Analysis of subcellularly localized mRNAs using *in situ* hybridization, mRNA amplification, and expression profiling. *Neurochem. Res.* **27,** 1065–1077 CrossRef Medline
37. Lein, E. S., Hawrylycz, M. J., Ao, N., Ayres, M., Bensinger, A., Bernard, A., Boe, A. F., Boguski, M. S., Brockway, K. S., Byrnes, E. J., Chen, L., Chen, L., Chen, T.-M., Chin, M. C., Chong, J., *et al.* (2007) Genome-wide atlas of gene expression in the adult mouse brain. *Nature* **445,** 168–176 CrossRef Medline
38. Muslimov, I. A., Nimmrich, V., Hernandez, A. I., Tcherepanov, A., Sacktor, T. C., and Tiedge, H. (2004) Dendritic transport and localization of protein kinase Mζ mRNA: implications for molecular memory consolidation. *J. Biol. Chem.* **279,** 52613–52622 CrossRef Medline
39. Zhong, J., Zhang, T., and Bloch, L. M. (2006) Dendritic mRNAs encode diversified functionalities in hippocampal pyramidal neurons. *BMC Neurosci.* **7,** 17–28 CrossRef Medline
40. Steward, O., and Schuman, E. M. (2001) Protein synthesis at synaptic sites on dendrites. *Annu. Rev. Neurosci.* **24,** 299–325 CrossRef Medline
41. Kratz, A., Beguin, P., Kaneko, M., Chimura, T., Suzuki, A. M., Matsunaga, A., Kato, S., Bertin, N., Lassmann, T., Vigot, R., Carninci, P., Plessy, C., and Launey, T. (2014) Digital expression profiling of the compartmentalized translatome of Purkinje neurons. *Genome Res.* **24,** 1396–1410 CrossRef Medline
42. Radeva, M. Y., Kugelmann, D., Spindler, V., and Waschke, J. (2014) PKA compartmentalization via AKAP220 and AKAP12 contributes to endothelial barrier regulation. *PLoS One* **9,** e106733 CrossRef Medline
43. GrandPré, T., Nakamura, F., Vartanian, T., and Strittmatter, S. M. (2000) Identification of the Nogo inhibitor of axon regeneration as a Reticulon protein. *Nature* **403,** 439–444 CrossRef Medline
44. Okazaki, T., Wang, H., Masliah, E., Cao, M., Johnson, S. A., Sundsmo, M., Saitoh, T., and Mori, N. (1995) SCG10, a neuron-specific growth-associated protein in Alzheimer's disease. *Neurobiol. Aging* **16,** 883–894 CrossRef Medline
45. Campbell, D. S., and Holt, C. E. (2001) Chemotropic responses of retinal growth cones mediated by rapid local protein synthesis and degradation. *Neuron* **32,** 1013–1026 CrossRef Medline
46. Piper, M., Anderson, R., Dwivedy, A., Weinl, C., van Horck, F., Leung, K. M., Cogill, E., and Holt, C. (2006) Signaling mechanisms underlying Slit2-induced collapse of *Xenopus* retinal growth cones. *Neuron* **49,** 215–228 CrossRef Medline
47. Condeelis, J., and Singer, R. H. (2005) How and why does β-actin mRNA target? *Biol. Cell* **97,** 97–110 CrossRef Medline
48. Yoon, B. C., Jung, H., Dwivedy, A., O'Hare, C. M., Zivraj, K. H., and Holt, C. E. (2012) Local translation of extranuclear lamin B promotes axon maintenance. *Cell* **148,** 752–764 CrossRef Medline
49. Ji, S.-J., and Jaffrey, S. R. (2012) Intra-axonal translation of SMAD1/5/8 mediates retrograde regulation of trigeminal ganglia subtype specification. *Neuron* **74,** 95–107 CrossRef Medline
50. Cox, L. J., Hengst, U., Gurskaya, N. G., Lukyanov, K. A., and Jaffrey, S. R. (2008) Intra-axonal translation and retrograde trafficking of CREB promotes neuronal survival. *Nat. Cell Biol.* **10,** 149–159 CrossRef Medline
51. Crino, P., Khodakhah, K., Becker, K., Ginsberg, S., Hemby, S., and Eberwine, J. (1998) Presence and phosphorylation of transcription factors

in developing dendrites. *Proc. Natl. Acad. Sci. U.S.A.* **95,** 2313–2318 CrossRef Medline

52. Barrett, L. E., Sul, J. Y., Takano, H., Van Bockstaele, E. J., Haydon, P. G., and Eberwine, J. H. (2006) Region-directed phototransfection reveals the functional significance of a dendritically synthesized transcription factor. *Nat. Methods* **3,** 455–460 CrossRef Medline
53. Lécuyer, E., Yoshida, H., Parthasarathy, N., Alm, C., Babak, T., Cerovina, T., Hughes, T. R., Tomancak, P., and Krause, H. M. (2007) Global analysis of mRNA localization reveals a prominent role in organizing cellular architecture and function. *Cell* **131,** 174–187 CrossRef Medline
54. Katz, Z. B., English, B. P., Lionnet, T., Yoon, Y. J., Monnier, N., Ovryn, B., Bathe, M., and Singer, R. H. (2016) Mapping translation "hot-spots" in live cells by tracking single molecules of mRNA and ribosomes. *Elife* **5,** e10415–e10430 Medline
55. Wang, C., Han, B., Zhou, R., and Zhuang, X. (2016) Real-time imaging of translation on single mRNA transcripts in live cells. *Cell* **165,** 990–1001 CrossRef Medline
56. Yan, X., Hoek, T. A., Vale, R. D., and Tanenbaum, M. E. (2016) Dynamics of translation of single mRNA molecules *in vivo*. *Cell* **165,** 976–989 CrossRef Medline
57. Wu, B., Eliscovich, C., Yoon, Y. J., and Singer, R. H. (2016) Translation dynamics of single mRNAs in live cells and neurons. *Science* **352,** 1430–1435 CrossRef Medline
58. Tcherkezian, J., Brittis, P. A., Thomas, F., Roux, P. P., and Flanagan, J. G. (2010) Transmembrane receptor DCC associates with protein synthesis machinery and regulates translation. *Cell* **141,** 632–644 CrossRef Medline
59. Weatheritt, R. J., Gibson, T. J., and Babu, M. M. (2014) Asymmetric mRNA localization contributes to fidelity and sensitivity of spatially localized systems. *Nat. Struct. Mol. Biol.* **21,** 833–839 CrossRef Medline
60. Gomes, C., Merianda, T. T., Lee, S. J., Yoo, S., and Twiss, J. L. (2014) Molecular determinants of the axonal mRNA transcriptome. *Dev. Neurobiol.* **74,** 218–232 CrossRef Medline
61. Taliaferro, J. M., Vidaki, M., Oliveira, R., Olson, S., Zhan, L., Saxena, T., Wang, E. T., Graveley, B. R., Gertler, F. B., Swanson, M. S., and Burge, C. B. (2016) Distal alternative last exons localize mRNAs to neural projections. *Mol. Cell* **61,** 821–833 CrossRef Medline
62. Dobin, A., Davis, C. A., Schlesinger, F., Drenkow, J., Zaleski, C., Jha, S., Batut, P., Chaisson, M., and Gingeras, T. R. (2013) STAR: ultrafast universal RNA-seq aligner. *Bioinformatics* **29,** 15–21 CrossRef Medline
63. Anders, S., Pyl, P. T., and Huber, W. (2015) HTSeq: a Python framework to work with high-throughput sequencing data. *Bioinformatics* **31,** 166–169 CrossRef Medline
64. Hulsen, T., de Vlieg, J., and Alkema, W. (2008) BioVenn: a web application for the comparison and visualization of biological lists using area-proportional Venn diagrams. *BMC Genomics* **9,** 488–494 CrossRef Medline
65. Huang da, W., Sherman, B. T., and Lempicki, R. A. (2009) Systematic and integrative analysis of large gene lists using DAVID bioinformatics resources. *Nat. Protoc.* **4,** 44–57 CrossRef Medline
66. Supek, F., Bošnjak, M., Škunca, N., and Šmuc, T. (2011) REVIGO summarizes and visualizes long lists of gene ontology terms. *PLoS One* **6,** e21800 CrossRef Medline
67. Wehrens, R., and Buydens, L. M. C. (2007) Self- and super-organising maps in R: the Kohonen package. *J. Stat. Softw.* **21,** 1–19